

# Microcalorimetric Studies on Chemical Oscillation of Microgels

Fang Zhao,<sup>†</sup> Yanwei Ding,<sup>†</sup> Yijie Lu,<sup>†</sup> Xiaoxia Liu,<sup>‡</sup> and Guangzhao Zhang<sup>\*,†</sup>

Hefei National Laboratory for Physical Sciences at Microscale, Department of Chemical Physics, University of Science and Technology of China, Hefei 230026, China, and Key Laboratory of Molecular Engineering of Polymers of Ministry of Education, Department of Macromolecular Science, Fudan University, Shanghai 200433, China

Received: January 20, 2009; Revised Manuscript Received: March 12, 2009

By use of isothermal titration calorimetry (ITC) and ultrasensitive differential scanning calorimetry (US-DSC), we have investigated the energy change in the periodic swelling-to-deswelling of thermally sensitive poly(*N*-isopropylacrylamide) (PNIPAM) microgels containing ruthenium(II) tris(2,2'-bipyridine) (Ru(bpy)<sub>3</sub>) which is a catalyst for Belousov–Zhabotinsky (BZ) reaction. As temperature increases, the induction period and oscillation period of BZ reaction decrease because the reaction rate increases. However, the oscillation disappears at a temperature above the lower critical solution temperature (LCST) of the microgels since Ru(bpy)<sub>3</sub> is trapped in the microgels and cannot react with BZ substrates. As microgel size increases or the cross-linking density decreases, the restriction of polymer networks on Ru(bpy)<sub>3</sub> decreases, so that Ru(bpy)<sub>3</sub> can readily contact with BZ substrates, leading the oscillation amplitude to increase. In addition, the so-called transient chaos occurs at a low stirring speed, and it wanes with the increasing stirring speed. All the facts indicate that the contact between Ru(bpy)<sub>3</sub> and BZ substrates determines the oscillation of the microgels.

## Introduction

Belousov–Zhabotinsky (BZ) reaction with rhythmical oscillation represents one of the nonequilibrium phenomena.<sup>1–3</sup> Considering that many physiological behaviors such as heartbeat and brainwaves exhibit oscillations, BZ reaction, especially those involving macromolecules, provides a model for understanding the biological phenomena.<sup>4,5</sup> Moreover, such reactions have found applications in nanodevices and intelligent materials.<sup>6</sup> Yoshida and co-workers<sup>7–13</sup> have developed a self-oscillating gel undergoing spontaneous swelling-to-deswelling volume transition without external stimuli under closed condition. Recently, they have also prepared BZ reaction induced oscillating microgels and investigated the oscillation by UV spectrum<sup>14–16</sup> and dynamic laser light scattering.<sup>17</sup> In such systems, chemical energy is converted into mechanical energy via BZ reaction. Note that the presence of macromolecules which can affect the diffusion and convection motion of BZ substrates usually makes the oscillation more complex.<sup>18–20</sup> Chaos, bursting, and pattern formation sometimes happen.<sup>20–23</sup> This is because an oscillation system generates a collective rhythm through mutual interactions, and a small local fluctuation can alter the oscillation behavior. So far, the oscillation dynamics remains largely unknown.

Calorimetry has been used to study BZ reactions involving small molecules.<sup>24–26</sup> Due to the low sensitivity of the conventional calorimetry, it provided limited information about the oscillation dynamics. Isothermal titration calorimetry (ITC) and ultrasensitive differential scanning calorimetry (US-DSC) are sensitive to detect the small energy change during a reaction or a physical change.<sup>27,28</sup> In the present study, we have prepared PNIPAM microgels containing Ru(bpy)<sub>3</sub> and investigated the energy change in the chemical oscillation by use of the

microcalorimetric techniques. The effects of temperature, stirring speed, cross-linking density, and size of microgels have been examined. Our aim is to understand the oscillation mechanism of a macromolecular system in terms of energy change.

## Experimental Section

**Materials.** *N*-Isopropylacrylamide (NIPAM) from Eastman Kodak was recrystallized three times from a benzene/hexane mixture prior to use. *N,N*-Methylenebisacrylamide (MBA) from Sinopharm was purified by recrystallization from methanol. Potassium persulfate (KPS) and azobis(isobutyronitrile) (AIBN) from Acros were recrystallized from deionized water and methanol, respectively. Hexafluorophosphate and *cis*-bis(2,2'-bipyridine)dichlororuthenium(II) dihydrate from Alpha, 4,4'-dimethyl-2,2'-bipyridine, and sodium dodecyl sulfate (SDS) from Sigma, malonic acid (MA, 99%), potassium bromate (99.8%), and nitric acid (68%) from Sinopharm were all used as received. All the solvents were distilled prior to use.

[Ruthenium (4-vinyl-4'-methyl-2,2'-bipyridine) bis(2,2'-bipyridine) bis(hexafluorophosphate)] (Ru(bpy)<sub>3</sub>) was synthesized following a reported procedure.<sup>29</sup> PNIPAM-Ru(bpy)<sub>3</sub> microgels were prepared by emulsion polymerization in water. Typically, NIPAM (0.501 g), Ru(bpy)<sub>3</sub> (0.025 g), SDS (0.038 g), and MBA (0.015 g) were dissolved in deionized water (50 mL) in a 100 mL three-necked flask, and KPS (0.031 g) in deionized water (2 mL) was introduced after the reactor was purged with bubbling nitrogen for 30 min. The mixture was stirred under nitrogen at 70 °C for 24 h. The unreacted monomer and surfactant were removed by dialysis against deionized water using a semipermeable membrane with a cutoff molar mass of 3000 g/mol. The freeze-drying of the solution yields microgel powder. The size and cross-linking density of the microgels were controlled by varying the molar ratio of SDS to MBA. PNIPAM-Ru(bpy)<sub>3</sub> without cross-linking was prepared in methanol following a similar procedure except that no MBA or SDS was

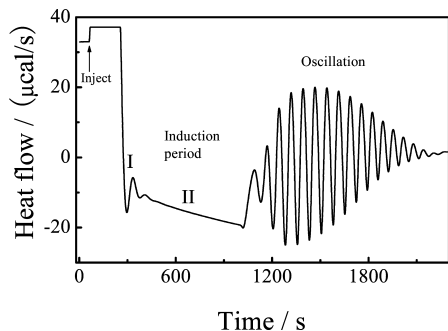
\* To whom correspondence should be addressed.

<sup>†</sup> University of Science and Technology of China.

<sup>‡</sup> Fudan University.

**TABLE 1: Characteristics of the Microgels at  $C_m = 1.0$  g/L**

	microgels					
	A	B	C	D	E	F
cross-linking density (mol %) <sup>a</sup>	12	8	4	2	2	2
$\langle R_h \rangle$ /nm	56	95	95	100	146	286
PDI	0.15	0.02	0.02	0.12	0.03	0.11

<sup>a</sup> Estimated from monomer feed ratio.**Figure 1.** Typical heat oscillation curve of the microgel A at 23 °C, where  $[\text{HNO}_3] = 380$  mM,  $[\text{MA}] = 67$  mM,  $[\text{KBrO}_3] = 61$  mM,  $C_m = 1.4$  g/L, and  $[\text{Ru}(\text{bpy})_3] = 6.5 \times 10^{-2}$  g/L.

added. Note that all Ru(II) ions are bound on the microgels due to the strong complex between Ru(II) and the bipyridines.<sup>14</sup>

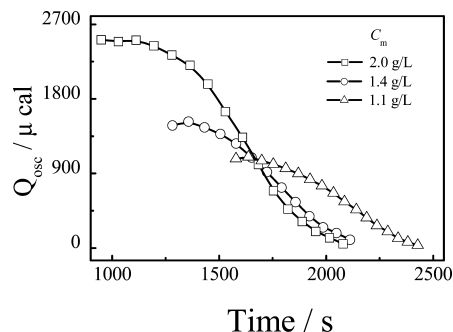
The hydrodynamic radius ( $\langle R_h \rangle$ ) and the distribution (PDI) of the microgels were determined by dynamic laser light scattering (DLS) on an ALV/DLS/SLS-5022F spectrometer at a concentration ( $C_m$ ) of 1.0 g/L (Table 1). The LCSTs of the microgels with Ru(II) and Ru(III) determined by DLS are 22 and 33 °C, respectively. The average molecular weight ( $M_w$ ) of the un-cross-linked polymer determined by static laser light scattering (SLS) is 140 000 g/mol. The concentration of Ru(bpy)<sub>3</sub> in microgels was determined by a Shimadzu-UV2401 spectrophotometer at the maximum wavelength of ~460 nm.

**ITC Measurements.** ITC measurements were carried out on a VP-ITC titration calorimeter (MicroCal, Inc.). All the solutions were thoroughly degassed before loading. The reference cell was filled with the deionized water. The sample cell was filled with the aqueous solution of the microgels, MA, and HNO<sub>3</sub>. The solution containing KBrO<sub>3</sub> and HNO<sub>3</sub> was placed in a 278 μL continuously stirred syringe. In the present study, all the experiments were performed in single injection mode (SIM). In parallel, a control experiment where no microgels but MA and HNO<sub>3</sub> were loaded in the sample cell was also conducted. All ITC experiments were done at 416 rpm to eliminate the effect of stirring unless otherwise specified. Data were analyzed by use of the software supplied by MicroCal. The quantity of heat ( $Q_{\text{osc}}$ ) of each oscillation was calculated by integrating the area of each peak after subtracting the baseline.

**US-DSC Measurements.** After the mixture of the microgels, HNO<sub>3</sub>, KBrO<sub>3</sub>, and MA solutions was quickly introduced to US-DSC cell, and the chemical oscillation without stirring was examined on a VP-DSC microcalorimeter (Microcal Inc.) under isothermal mode at 23 °C with deionized water as the reference.

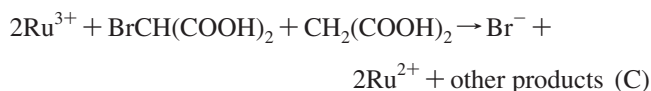
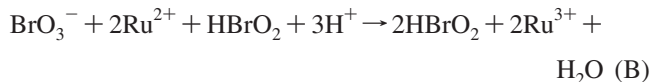
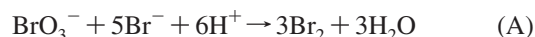
## Results and Discussion

Figure 1 shows a typical heat oscillation curve of the microgel solution at 23 °C. After a marked heat absorption due to the dilution of substrates, the heat flow sharply drops at about 255 s, indicating the reaction has undergone induction period. It is known that such a reaction involves two steps; that is, MA reacts

**Figure 2.** Time dependence of quantity of heat ( $Q_{\text{osc}}$ ) of each oscillation at different microgel concentrations (A) at 23 °C, where  $[\text{HNO}_3] = 380$  mM,  $[\text{MA}] = 67$  mM, and  $[\text{KBrO}_3] = 61$  mM.

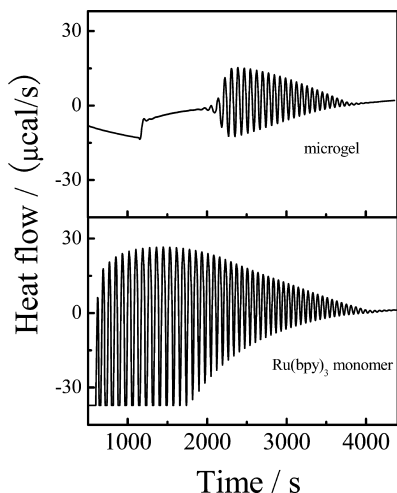
with the catalyst (step I) and then yields bromomalonic acid (BrMA) (step II).<sup>30</sup> Only when BrMA reaches a critical concentration<sup>31</sup> can the oscillation occur. The distinct heat oscillation indicates a periodic exothermic reaction. The oscillation period defined as an average time over five oscillations is 74 s, where the microgels undergo a mechanical volume oscillation.<sup>14–16</sup>

Figure 2 shows the amplitude reflecting the quantity of heat ( $Q_{\text{osc}}$ ) in each oscillation decays with time. This is understandable because the reaction is carried out under closed condition. With the gradual consumption of the substrates, the reaction decays and finally reaches a steady state. Since the reaction rate increases with the concentration of Ru(bpy)<sub>3</sub>, the induction period decreases with the concentration of the microgels. In addition, the oscillation period increases with the microgel concentration. It is well-known that each oscillation involves three processes following the Field–Körös–Noyes (FKN) mechanism;<sup>32</sup> that is



As the concentration of Ru(bpy)<sub>3</sub> increases, more Br<sup>−</sup> results, and the transition time between Ru(II) and Ru(III) increases, leading the oscillation period to increase. The heat ( $Q_{\text{osc}}$ ) in each oscillation also increases with microgel concentration. As we know, the heat in the reaction mainly evolves in processes B and C involving Ru(bpy)<sub>3</sub>.<sup>33</sup> Thus, the reaction rate increases with Ru(bpy)<sub>3</sub>, giving off more heat especially at the initial stage of the oscillation. Note that the initial substrate concentration can also affect the induction period, oscillation period, and amplitudes.<sup>14</sup> In the present study, we fixed the substrate concentration to eliminate the effect.

Figure 3 shows the chemical oscillation of Ru(bpy)<sub>3</sub> monomer in comparison with microgels, where the concentrations ( $3 \times 10^{-2}$  g/L) of Ru(bpy)<sub>3</sub> in them are the same. Clearly, Ru(bpy)<sub>3</sub> monomer exhibits an amplitude larger than that of the microgels. As reported before,<sup>14</sup> the microgels undergo a deswelling-to-swelling volume change in process B but a swelling-to-deswelling volume change in process C. Thus, the chemical energy of BZ reaction is converted into mechanical energy during the oscillation. Actually, the oscillation proceeds where the catalyst is spatially available.<sup>18</sup> Since the network confines the diffusion of substrate into the microgels, less heat is released



**Figure 3.** Time dependence of heat flow for microgel D and  $\text{Ru}(\text{bpy})_3$  monomer, where  $[\text{HNO}_3] = 380 \text{ mM}$ ,  $[\text{MA}] = 67 \text{ mM}$ ,  $[\text{KBrO}_3] = 61 \text{ mM}$ , and  $[\text{Ru}(\text{bpy})_3] = 3.0 \times 10^{-2} \text{ g/L}$ .

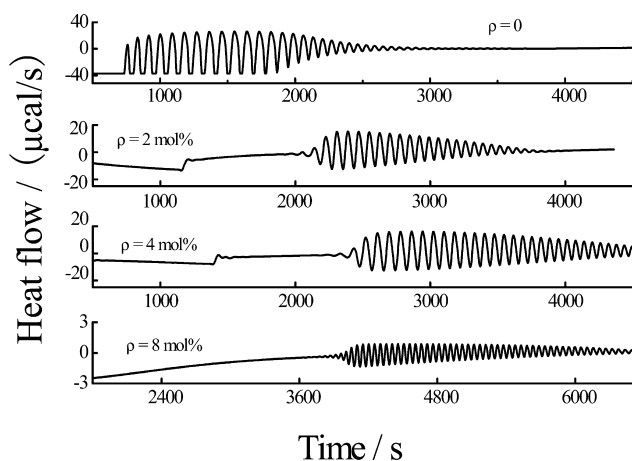


**Figure 4.** Time dependence of heat flow for the microgels with different cross-linking densities ( $\rho$ ) at  $23^\circ\text{C}$ , where  $[\text{HNO}_3] = 380 \text{ mM}$ ,  $[\text{MA}] = 67 \text{ mM}$ ,  $[\text{KBrO}_3] = 61 \text{ mM}$ , and  $[\text{Ru}(\text{bpy})_3] = 3.0 \times 10^{-2} \text{ g/L}$ .

in the microgels in comparison with a system involving only small molecules, so that a smaller amplitude is observed in the former. Parallely, due to the restriction of the polymer network, the reaction rate decreases, resulting in a longer induction period for the microgels.  $\text{Ru}(\text{bpy})_3$  monomer also exhibits a longer oscillation period than the microgels. Following the FKN mechanism,<sup>14</sup> we know that less  $\text{Br}^-$  resulted in the case of microgels because only part of the  $\text{Ru}(\text{bpy})_3$  immobilized in the microgels can participate in the reaction, so Process A corresponding to the consumption of  $\text{Br}^-$  takes a shorter time. Note that the transition time between  $\text{Ru}(\text{II})$  and  $\text{Ru}(\text{III})$  may be prolonged due to the poor diffusion of the substrates in microgels. That is, the duration for processes B and C increases but the duration for process A decreases. However, the combination of the effects generally leads to the oscillation period to decrease. This is in agreement with the previous results.<sup>14</sup>

Figure 4 shows that the induction period increases but the oscillation period and amplitude decrease as the cross-linking density ( $\rho$ ) of the microgels increases. This is because the substrates are more difficult to diffuse into microgels at a higher cross-linking density. Thus, it takes more time for the reactions to yield enough  $\text{BrMA}$  in the induction period. On the other hand,  $\text{Ru}(\text{bpy})_3$  confined in the microgels is difficult to contact

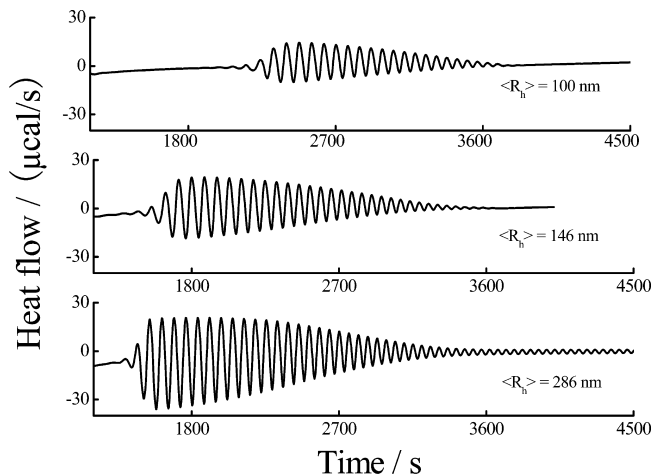


**Figure 5.** Time dependence of heat flow for the microgels with different sizes at  $23^\circ\text{C}$ , where  $[\text{HNO}_3] = 380 \text{ mM}$ ,  $[\text{MA}] = 67 \text{ mM}$ ,  $[\text{KBrO}_3] = 61 \text{ mM}$ , and  $[\text{Ru}(\text{bpy})_3] = 3.0 \times 10^{-2} \text{ g/L}$ .

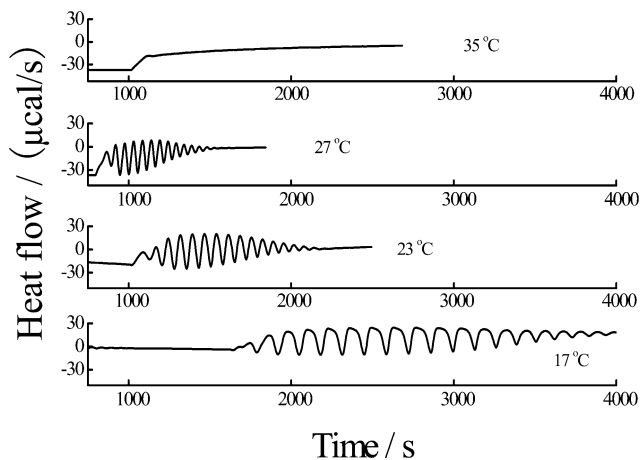
with BZ substrates, so less heat is released. Moreover, since the cross-linking restricts  $\text{Ru}(\text{bpy})_3$  from participating in the BZ reaction, the oscillation period decreases with the cross-linking density. PNIPAM- $\text{Ru}(\text{bpy})_3$  without cross-linking has an oscillation period somewhat longer than that of  $\text{Ru}(\text{bpy})_3$  monomer, indicating that un-cross-linked polymer chains can also confine the motion of the catalyst. The presence of PNIPAM- $\text{Ru}(\text{bpy})_3$  can also increase the viscosity of the solution,<sup>21</sup> further decreasing the diffusion of the substrates. That is why PNIPAM- $\text{Ru}(\text{bpy})_3$  exhibits a longer oscillation period. Besides,  $\text{Ru}(\text{bpy})_3$  monomer exhibits an oscillation duration much longer than that of the microgels. This is because some  $\text{Ru}(\text{bpy})_3$  are trapped in the microgels and cannot react with substrates.

Figure 5 shows the effect of size on the oscillation of the microgels with a cross-linking density of 2 mol %, which have the same concentration of  $\text{Ru}(\text{bpy})_3$ . It can be seen that as the size of the microgels increases, the induction period and oscillation period decrease but the amplitude increases. It is known that a larger microgel can contain more  $\text{Ru}(\text{bpy})_3$ , namely, the local concentration of  $\text{Ru}(\text{bpy})_3$  is higher in a larger microgel dispersion. On the other hand, larger microgels with a thicker wall can reduce the dissipation and the deactivation of the autocatalytic species.<sup>18</sup> Thus, the BZ substrates have more chances to contact with  $\text{Ru}(\text{bpy})_3$ , leading to more reaction heat or a larger amplitude. For the same reason, the oscillation period decreases with microgel size. Clearly, the contact between the catalyst and substrates plays a critical role in the chemical oscillation involving macromolecules. Accordingly, by regulating the cross-linking density and size of the microgels, the oscillation period and amplitude can be tuned.

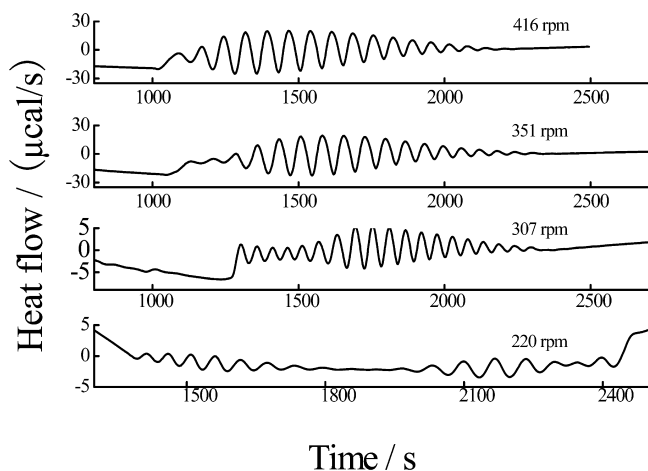
Figure 6 shows the effect of temperature on the oscillation of the microgels. At a temperature below the LCST of the microgels with  $\text{Ru}(\text{III})$  ( $\sim 33^\circ\text{C}$ ), the induction period and oscillation period decrease with temperature. This is because the substrates can react more readily at a higher temperature, leading to shorter oscillation duration. The activation energy of oscillation estimated with Arrhenius equation is  $67.2 \text{ kJ/mol}$  here, which is consistent with the previous result.<sup>34</sup>

Figure 6 also shows that the oscillation disappears above  $33^\circ\text{C}$ . It is reported that the mechanical oscillation can only happen at a temperature between the LCSTs of the microgels with  $\text{Ru}(\text{II})$  and  $\text{Ru}(\text{III})$ .<sup>7</sup> As stated above, the polymer network restricts  $\text{Ru}(\text{bpy})_3$  from contacting with BZ substrates. At a temperature above the LCST of the microgels with  $\text{Ru}(\text{III})$  ( $\sim 33^\circ\text{C}$ ), the aggregation of the microgels further builds up such a restriction.





**Figure 6.** Time dependence of heat flow for the microgel A at different temperatures, where  $[\text{HNO}_3] = 380 \text{ mM}$ ,  $[\text{MA}] = 67 \text{ mM}$ ,  $[\text{KBrO}_3] = 61 \text{ mM}$ ,  $C_m = 1.4 \text{ g/L}$ , and  $[\text{Ru}(\text{bpy})_3] = 6.5 \times 10^{-2} \text{ g/L}$ .



**Figure 7.** Time dependence of heat flow for the microgel A at different stirring speeds at  $23^\circ\text{C}$ , where  $[\text{HNO}_3] = 380 \text{ mM}$ ,  $[\text{MA}] = 67 \text{ mM}$ ,  $[\text{KBrO}_3] = 61 \text{ mM}$ ,  $C_m = 1.4 \text{ g/L}$ , and  $[\text{Ru}(\text{bpy})_3] = 6.5 \times 10^{-2} \text{ g/L}$ .

Consequently, the chemical oscillation is completely suppressed. However, we found that the heat oscillation occurs at a temperature below the LCST of the microgels with  $\text{Ru}(\text{II})$  ( $\sim 22^\circ\text{C}$ ). It is known that the heat is mainly generated from the BZ reaction. Since the microgels are swollen at a temperature below  $\sim 22^\circ\text{C}$ , where  $\text{Ru}(\text{bpy})_3$  can readily contact and react with the substrates, the heat oscillation can still happen even though the mechanical oscillation stops.

Figure 7 shows the induction period and oscillation period increase as stirring speed decreases. As discussed above, this is because of the poor contact between the catalyst and substrates under slow stirring. Particularly, when the speed is below 220 rpm, a transient chaotic oscillation can be observed. Such a phenomenon has been attributed to the interplay between chemical kinetics of BZ reaction and diffusion–convection process.<sup>21</sup> Further increasing the speed leads the amplitude to increase and even level off at a speed above 351 rpm. This indicates that the catalyst can efficiently contact and react with the BZ substrates under vigorous stirring.

To have better understanding of the transient chaos, we also investigated the chemical oscillation without stirring by use of US-DSC. Figure 8 shows that aperiodic oscillation indeed occurs, particularly at a high concentration of microgels. It can be discerned more clearly in the inset. Such a phenomenon has also been observed in  $\text{Ce}(\text{IV})$ -catalyzed BZ reaction.<sup>22</sup> It is

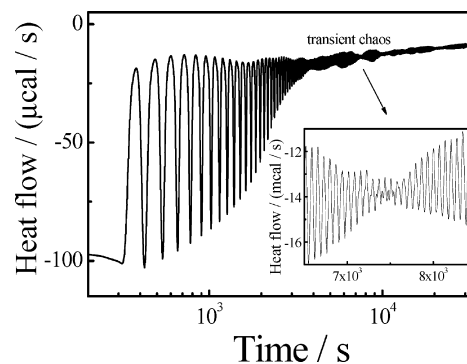


**Figure 8.** Time dependence of heat flow for the microgel A under a condition without stirring, where  $[\text{HNO}_3] = 400 \text{ mM}$ ,  $[\text{MA}] = 56 \text{ mM}$ ,  $[\text{KBrO}_3] = 72 \text{ mM}$ ,  $C_m = 5.8 \text{ g/L}$ , and  $[\text{Ru}(\text{bpy})_3] = 0.26 \text{ g/L}$ . The inset shows the transient chaos in a large scale.

known that every two periodic oscillations are separated by an aperiodic transient regime. Since the microgels were already well mixed with the substrates prior to the measurement, the aperiodic oscillation should be triggered by the contact between the catalyst and the substrates. Actually, convection is one of the bifurcation parameters for chaos in such systems. When it is coupled with diffusion and chemical kinetics, the onset of chaos occurs.<sup>21</sup> In a BZ reaction without stirring, the convection arises from the difference of density and the thermal gradient. In our preliminary experiments, we found that a high temperature (below  $\sim 33^\circ\text{C}$ ) favors the diffusion of substrates and brings less irregular oscillation. Therefore, the transient chaos is due to the thermal gradient and density fluctuation in the present system. Anyway, the reaction ultimately reaches thermodynamic equilibrium, and the chaotic oscillation is spatiotemporal transient and disappears with time.

## Conclusions

Isothermal titration calorimetry (ITC) and ultrasensitive differential scanning calorimetry (US-DSC) are sensitive to detect chemical oscillation. The oscillation of microgels containing a catalyst for BZ reaction is influenced by temperature, stirring, cross-linking density, and size of microgels. The PNIPAM network restricts the catalyst from contacting and reacting with the BZ substrates and hence affects the oscillation period, oscillation amplitude, and induction period. At a temperature below the lower critical solution temperature (LCST), the chemical oscillation becomes acute as temperature increases. However, the oscillation disappears at a temperature above the LCST. Stirring can profoundly influence the contact between the catalyst and the substrates, and transient chaos can be observed at a low stirring speed. The parameters for oscillation of the microgels can be tuned by regulating the above factors. The microgels may find applications in nanomachines, biosensors, and drug delivery.

**Acknowledgment.** The financial support of National Natural Science Foundation (NNSF) of China (20474060 and 20611120039) and Ministry of Science and Technology of China (2007CB936401) is acknowledged.

## References and Notes

- (1) Zaikin, A. N.; Zhabotinsky, A. M. *Nature (London)* **1970**, 225, 535.
- (2) Noszticzius, Z.; Gaspar, V.; Foersterling, H. D. *J. Am. Chem. Soc.* **1985**, 107, 2314.
- (3) Zhang, C. X.; Liao, H. M.; Zhou, L. Q.; Ouyang, Q. *Phys. Chem. B* **2004**, 108, 16990.

- (4) Kuhnert, L.; Agladze, K. I.; Krinsky, V. I. *Nature (London)* **1989**, 337, 244.
- (5) Castets, V.; Dulos, E.; Boissonade, J.; De Kepper, P. *Phys. Rev. Lett.* **1990**, 64, 2953.
- (6) Maeda, S.; Hara, Y.; Sakai, T.; Yoshida, R.; Hashimoto, S. *Adv. Mater.* **2007**, 19, 3480.
- (7) Yoshida, R.; Takahashi, T.; Yamaguchi, T.; Ichijo, H. *J. Am. Chem. Soc.* **1996**, 118, 5134.
- (8) Yoshida, R.; Tanaka, M.; Onodera, S.; Yamaguchi, T.; Kokufuta, E. *J. Phys. Chem. A* **2000**, 104, 7549.
- (9) Yoshida, R.; Takei, K.; Yamaguchi, T. *Macromolecules* **2003**, 36, 1759.
- (10) Sasaki, S.; Koga, S.; Yoshida, R.; Yamaguchi, T. *Langmuir* **2003**, 19, 5595.
- (11) Takeoka, Y.; Watanabe, M.; Yoshida, R. *J. Am. Chem. Soc.* **2003**, 125, 13320.
- (12) Sakai, T.; Hara, Y.; Yoshida, R. *Macromol. Rapid Commun.* **2005**, 26, 1140.
- (13) Yoshida, R.; Sakai, T.; Ito, S.; Yamaguchi, T. *J. Am. Chem. Soc.* **2002**, 124, 8095.
- (14) Suzuki, D.; Yoshida, R. *J. Phys. Chem. B* **2008**, 112, 12618.
- (15) Hara, Y.; Yoshida, R. *J. Phys. Chem. B* **2005**, 109, 9451.
- (16) Suzuki, D.; Yoshida, R. *Macromolecule* **2008**, 41, 5830.
- (17) Sakai, T.; Yoshida, R. *Langmuir* **2004**, 20, 1036.
- (18) Yoshikawa, K.; Aihara, R.; Agladze, K. *J. Phys. Chem. A* **1998**, 102, 7649.
- (19) Yamaguchi, T.; Kuhnert, L.; Nagy-Ungvarai, Z.; Mueller, S. C.; Hess, B. *J. Phys. Chem.* **1991**, 95, 5831.
- (20) Agladze, K.; Dulos, E.; De Kepper, P. *J. Phys. Chem.* **1992**, 96, 2400.
- (21) Turco Liveri, M. L.; Lombardo, R.; Masia, M.; Calvaruso, G.; Rustici, M. *J. Phys. Chem. A* **2003**, 107, 4834.
- (22) Marchettini, M.; Rustici, M. *Chem. Phys. Lett.* **2000**, 317, 647.
- (23) Rustici, M.; Caravati, C.; Petretto, E.; Branca, M.; Marchettini, N. *J. Phys. Chem. A* **1999**, 103, 6564.
- (24) Agreda, J.; Barragán, D.; Gómez, A. *J. Therm. Anal. Cal.* **2003**, 74, 875.
- (25) Nagy, G.; Körös, E.; Lamprecht, I. *J. Therm. Anal. Cal.* **1999**, 57, 209.
- (26) Sun, H.; Wang, X.; Liu, Y.; Nan, Z.; Zhang, H. *J. Therm. Anal. Cal.* **1999**, 58, 117.
- (27) Tam, K. C.; Wang, C.; Jenkins, R. D. *J. Phys. Chem. B* **2002**, 106, 1195.
- (28) Yaroslavov, A. A.; Sitnikova, T. A.; Rakhnyanskaya, A. A.; Ermakov, Y. A.; Burova, T. V.; Grinberg, V. Y.; Menger, F. M. *Langmuir* **2007**, 23, 7539.
- (29) Ghosh, P.; Spiro, T. G. *J. Am. Chem. Soc.* **1980**, 102, 5543.
- (30) Kawahito, J.; Fujieda, S. *Thermochim. Acta* **1992**, 210, 1.
- (31) Sirimungkala, A.; Forsterling, H. D.; Dlask, V.; Field, R. J. *J. Phys. Chem. A* **1999**, 103, 1038.
- (32) Field, R. J.; Körös, E.; Noyes, R. M. *J. Am. Chem. Soc.* **1972**, 94, 8649.
- (33) Fujieda, S.; Kawahito, J. *Thermochim. Acta* **1991**, 183, 153.
- (34) Nagy, G.; Körös, E.; Oftedal, N.; Tjellflaat, K.; Ruoff, P. *Chem. Phys. Lett.* **1996**, 250, 255.

JP9006203